

**NEWTON, Volume 1**

**Supplemental information**

**Revealing chain scission modes  
in variable polymer degradation kinetics**

**Yijie Cheng, Adolfo Lopez, Tsz Hung Wong, Darryl Francis, Emily England, and Xinyue Liu**

## **Supplemental Information**

This PDF file includes:

### **1. Supplemental Notes**

Note S1. Moment analysis for molecular weight distribution of polymers.  
Note S2. Mathematical modeling for chain-end scission.  
Note S3. Mathematical modeling for random scission.  
Note S4. Calculation of the degradable bond fraction.

### **2. Supplemental Figures**

Figure S1. Fitting polymer degradation data to chain scission modes.  
Figure S2. Time evolution of normalized molar and mass concentrations under chain-end scission.  
Figure S3. Time evolution of normalized molar and mass concentrations under random scission.  
Figure S4. Pearson correlation analysis of polymer crystallinity with chain scission preference.  
Figure S5. Chemical structures of repeat units in polylactic acid and citrus pectin.

### **3. Supplemental Tables**

Table S1. Summary of different polymer degradation with chain scission fitting and polymer characteristics.  
Table S2. Summary of different polymer degradation with chain scission fitting and polymer crystallinity.

### **4. Supplemental References**

## Supplemental Notes

### Note S1. Moment analysis for molecular weight distribution of polymers.

To describe the time evolution of molecular weight (MW) distributions during polymer degradation, we define  $P(x, t)$  as the time-dependent chain length distribution function, where  $P(x, t)dx$  represents the molar concentration of polymer chains with lengths between  $x$  and  $x + dx$  at time  $t$ . The time evolution of the chain length (that is, degree of polymerization, DOP) distribution is governed by the population balance equation, given by  $dP(x, t)/dt = F(x) - D(x)$ , where  $F(x)$  is the formation of polymer chains of length  $x$  (e.g., from scission of longer chains), and  $D(x)$  accounts for their depletion (e.g., through further cleavage). We assume that the reaction rate constant for a specific chain scission,  $k$ , is independent of chain length and time.

Solving rate expressions of chain length distributions  $dP(x, t)/dt$  leads to not only numerical solutions of the time-evolving chain length distribution  $P(x, t)$ , but also analytic solutions of averaged properties of the chain length distributions  $P^{(n)}(t)$  by using the method of moments in statistics. The moments of the chain length distributions are defined as the integrals over the chain length,  $x$ ,

$$P^{(n)}(t) = \int_0^{\infty} P(x, t) x^n dx, \quad (\text{Equation S1})$$

where the superscript  $n$  is the moment order. When  $n = 0$ , the zeroth moment  $P^{(0)}(t)$  is the total molar concentration of the *polymer*  $c_{\text{mole}}(t)$  in the unit of mol/volume. When  $n = 1$ , the first moment  $P^{(1)}(t)$  is the total molar concentration of the repeat units in the polymer in the unit of mol/volume. The product of the first moment and the molecular weight of a repeat unit,  $P^{(1)}(t) \text{ MW}_1$ , represents the mass concentration of the polymer  $c_{\text{mass}}(t)$  in the unit of mass/volume. Therefore, the number-average MW at time  $t$  is given by

$$\overline{\text{MW}(t)} = P^{(1)}(t) \text{ MW}_1 / P^{(0)}(t) = c_{\text{mass}}(t) / c_{\text{mole}}(t). \quad (\text{Equation S2})$$

At the initial time,  $t = 0$ , the number-average MW is

$$\overline{\text{MW}(0)} = P^{(1)}(0) \text{ MW}_1 / P^{(0)}(0) = c_{\text{mass}}(0) / c_{\text{mole}}(0). \quad (\text{Equation S3})$$

## Note S2. Mathematical modeling for chain-end scission.

We adopt the mathematical framework developed by McCoy et al.[S1,2] to analyze the time evolution of polymer MW distributions when subjected to chain-end scission. In this degradation mode, cleavage occurs exclusively at the terminal end of the polymer chain and generates monomers. The general chain scission reaction is expressed as



where a polymer molecule of initial chain length  $x_0$  breaks into two product molecules: a polymer fragment of length  $(x_0 - 1)$  and a monomer unit of length 1.

### 1. Population balance equations for chain length distribution

The overall chain length distribution  $P(x, t)$  under random scission follows the population balance equation  $P(x, t) = p(x, t) + q(1, t)$  and is divided into two categories below.

(i) For non-monomers ( $x > 1$ ), the population balance equation is given by

$$dp(x, t)/dt = -kp(x, t) + kp(x + 1, t), \quad (\text{Equation S5})$$

where the first term  $-kp(x, t)$  describes the depletion rate of polymer chains of length  $x$  due to cleavage, and the second term  $kp(x + 1, t)$  accounts for the formation rate of polymer chains of length  $x$  from the degradation of longer chains ( $x + 1$ ).

(ii) For the monomer products ( $x = 1$ ) which are only formed but not further degraded, the population balance equation is

$$dq(1, t)/dt = k \int_0^\infty p(x, t) dx. \quad (\text{Equation S6})$$

### 2. Moment analysis for MW evolution

To derive analytical solutions for MW evolution, we apply the moment operation  $\int_0^\infty f(x) x^n dx$  to both sides of the governing equations (Equations S5 and S6).

#### (ii) Moments for non-monomers

Applying the moment operation to Equation S5, we obtain

$$\frac{d}{dt} \int_0^\infty p(x, t) x^n dx = -k \int_0^\infty p(x, t) x^n dx + k \int_0^\infty p(x + 1, t) x^n dx. \quad (\text{Equation S7})$$

The left-hand side simplifies to

$$\frac{d}{dt} \int_0^\infty p(x, t) x^n dx = dp^{(n)}(t)/dt, \quad (\text{Equation S8})$$

where  $p^{(n)}(t)$  is the nth moment of the chain length distribution.

For the first term on the right-hand side, we obtain

$$-k \int_0^\infty p(x, t) x^n dx = -kp^{(n)}(t) \quad (\text{Equation S9})$$

For the second term on the right-hand side, we perform a variable substitution from  $x$  to  $x + 1$ , leading to

$$k \int_0^\infty p(x + 1, t) x^n dx = k \int_0^\infty p(x + 1, t) [(x + 1) - 1]^n d(x + 1). \quad (\text{Equation S10})$$

Using the binomial expansion

$$[(x + 1) - 1]^n = \sum_{j=0}^n \binom{n}{j} (-1)^{n-j} (x + 1)^j, \quad (\text{Equation S11})$$

we rewrite Equation S10 as

$$k \int_0^\infty p(x + 1, t) [(x + 1) - 1]^n d(x + 1) = k \sum_{j=0}^n \binom{n}{j} (-1)^{n-j} \int_0^\infty p(x + 1, t) (x + 1)^j d(x + 1). \quad (\text{Equation S12})$$

Since the integral form of moments is defined as  $p^{(j)}(t) = \int_0^\infty p(x, t) x^j dx$ , we simplify Equation S12 to

$$k \sum_{j=0}^n \binom{n}{j} (-1)^{n-j} \int_0^\infty p(x + 1, t) (x + 1)^j d(x + 1) = k \sum_{j=0}^n \binom{n}{j} (-1)^{n-j} p^{(j)}(t). \quad (\text{Equation S13})$$

Combining Equations S7, S8 and S13, we can derive the general rate expression for moment evolution as

$$dp^{(n)}(t)/dt = -kp^{(n)}(t) + k \sum_j \binom{n}{j} (-1)^{n-j} p^{(j)}(t). \quad (\text{Equation S14})$$

When  $n = 0$ , we evaluate the summation term in Equation S14

$$\sum_{j=0}^0 \binom{0}{j} (-1)^{0-j} p^{(j)}(t) = p^{(0)}(t). \quad (\text{Equation S15})$$

This implies

$$dp^{(0)}(t)/dt = -kp^{(n)}(t) + kp^{(n)}(t) = 0. \quad (\text{Equation S16})$$

Thus, the zeroth moment  $p^{(0)}(t)$  remains constant over time

$$p^{(0)}(t) = p^{(0)}(0). \quad (\text{Equation S17})$$

Since the initial condition of  $p^{(0)}(0)$  is equal to the initial molar concentration of polymer chains  $c_{\text{mole}}(0)$ , we obtain

$$p^{(0)}(t) = c_{\text{mole}}(0). \quad (\text{Equation S18})$$

When  $n = 1$ , we evaluate

$$\sum_{j=0}^1 \binom{1}{j} (-1)^{1-j} p^{(j)}(t) = -p^{(0)}(t) + p^{(1)}(t). \quad (\text{Equation S19})$$

Substituting this into Equation S14 gives

$$dp^{(1)}(t)/dt = -kp^{(1)}(t) + k(-p^{(0)}(t) + p^{(1)}(t)) = -kp^{(0)}(t). \quad (\text{Equation S20})$$

Since the zeroth moment is constant over time, i.e.,  $p^{(0)}(t) = p^{(0)}(0)$ , we simplify

$$dp^{(1)}(t)/dt = -kp^{(0)}(0). \quad (\text{Equation S21})$$

Thus, the first moment  $p^{(1)}(t)$  decrease linearly over time

$$p^{(1)}(t) = p^{(1)}(0) - p^{(0)}(0)kt. \quad (\text{Equation S22})$$

Since the initial condition of  $p^{(1)}(0) = c_{\text{mass}}(0)/\text{MW}_1$  and  $p^{(0)}(0) = c_{\text{mole}}(0)$ , we can obtain

$$p^{(1)}(t) = c_{\text{mass}}(0)/\text{MW}_1 - c_{\text{mole}}(0)kt. \quad (\text{Equation S23})$$

## (ii) Moments for monomer products

The above calculations consider the non-monomers with chain lengths ranging from 2 to a maximum value ( $x > 1$ ). To fully describe the system, we also need to consider the MW distribution for monomer products denoted as  $q(x, t)$  when  $x = 1$ . We notice that the right side in the monomer rate expression in Equation S6 can be rewritten in moment form as

$$k \int_0^\infty p(x, t) dx = kp^{(0)}(t). \quad (\text{Equation S24})$$

Substituting this into Equation S6, we obtain

$$dq(1, t)/dt = kp^{(0)}(t). \quad (\text{Equation S25})$$

Since the zeroth moment remains constant over time, i.e.,

$$p^{(0)}(t) = c_{\text{mole}}(0), \quad (\text{Equation S26})$$

integrating both sides of Equation S25 yields

$$q(1, t) = c_{\text{mole}}(0)kt. \quad (\text{Equation S27})$$

Since monomers consistently have a chain length of 1, their corresponding moment expressions are

$$q^{(0)}(t) = c_{\text{mole}}(0)kt, \quad (\text{Equation S28})$$

and

$$q^{(1)}(t) = c_{\text{mole}}(0)kt. \quad (\text{Equation S29})$$

## 3. Number-average molecular weight

The total molar concentration is obtained by summing the zeroth moments of both non-monomers ( $x > 1$ ) from Equation S18 and monomers from Equation S28 as

$$c_{\text{mole}}(t) = p^{(0)}(t) + q^{(0)}(t), \quad (\text{Equation S30})$$

which further gives

$$c_{\text{mole}}(t) = c_{\text{mole}}(0)(1 + kt). \quad (\text{Equation S31})$$

The total mass concentration is determined by summing the first moments of both non-monomers ( $x > 1$ ) from Equation S23 and monomers from Equation S29

$$c_{\text{mass}}(t)/\text{MW}_1 = p^{(1)}(t) + q^{(1)}(t). \quad (\text{Equation S32})$$

Multiplying the Equation S31 by  $\text{MW}_1$ , we will obtain the total mass concentration

$$c_{\text{mass}}(t) = c_{\text{mass}}(0). \quad (\text{Equation S33})$$

It indicates that the total mass is conserved throughout the degradation process. The average MW of all molecules is defined as the ratio of total mass concentration to total molar concentration, that is,

$$\overline{\text{MW}(t)} = \overline{\text{MW}(0)/(1 + kt)}. \quad (\text{Equation S34})$$

This expression provides a mathematical description of MW decay kinetics under chain-end scission. Additionally, we plot the normalized molar concentrations and normalized mass concentrations over time in **Figure S2A,B**, based on the above time-dependent expressions for both monomers and non-monomers. For the graphs in **Figure 2B-D** and **Figure S2A,B**, we assume the following values for a polydisperse polymer sample:  $c_{\text{mole}}(0) = 1 \text{ mmol L}^{-1}$ ,  $c_{\text{mass}}(0) = 5 \text{ g L}^{-1}$ ,  $\text{MW}_1 = 100 \text{ g mol}^{-1}$ .

### Note S3. Mathematical modeling for random scission.

We continue to adopt the mathematical framework developed by McCoy et al.[S1] to analyze the time evolution of MW distributions during random chain scission. Unlike chain-end scission, where cleavage occurs exclusively at the terminal bonds, random scission assumes that all backbone bonds are equally susceptible to cleavage. This results in a fragmentation process where long polymer chains randomly break into smaller fragments with varying sizes. The reaction for a polymer chain of initial length  $x_0$  undergoing random scission can be expressed as



where  $x_1$  represents the length of a newly generated polymer fragment, and  $(x_0 - x_1)$  is the remaining polymer segment. This process continues sequentially, further fragmenting the polymer chains over time, with the general reaction expressed as



where the subscript  $j$  is a serial number of degradation reactions.

#### 1. Population balance equations for chain length distribution

The overall chain length distribution  $P(x, t)$  under random scission follows the population balance equation  $P(x, t) = p(x, t) + q(x, t) + r(x, t)$  and is divided into three categories below.

(i) For undegraded reactants ( $x = x_0$ ), only depletion occurs:

$$dp(x, t)/dt = -kp(x, t). \quad (\text{Equation S37})$$

(ii) For intermediate products ( $1 < x < x_0$ ), both depletion and formation terms exist:

$$dq(x, t)/dt = -kq(x, t) + 2k \int_x^\infty \frac{q(x_i, t)}{x_i} dx_i. \quad (\text{Equation S38})$$

(iii) For final products ( $x = 1$ ), only formation occurs:

$$dr(x, t)/dt = 2k \int_x^\infty \frac{r(x_i, t)}{x_i} dx_i. \quad (\text{Equation S39})$$

#### 2. Moment analysis for MW evolution

To derive analytical solutions for MW evolution, we apply the moment operation  $\int_0^\infty f(x) x^n dx$  to both sides of the governing equations (Equations S37-39).

##### (i) Moments for undegraded reactants

For the undegraded reactants ( $x = x_0$ ), we will apply moment operation to both sides of Equation S37, yielding the moment equation

$$\frac{d}{dt} \int_0^\infty p(x, t) x^n dx = -k \int_0^\infty p(x, t) x^n dx, \quad (\text{Equation S40})$$

which simplifies to

$$dp^{(n)}(t)/dt = -kp^{(n)}(t). \quad (\text{Equation S41})$$

With the initial conditions  $p^{(0)}(0) = c_{\text{mole}}(0)$  and  $p^{(1)}(0) = c_{\text{mass}}(0)/\text{MW}_1$ , we can solve the zeroth and first moments to be

$$p^{(0)}(t) = c_{\text{mole}}(0)e^{-kt}, \quad (\text{Equation S42})$$

and

$$p^{(1)}(t) = c_{\text{mass}}(0)e^{-kt}/\text{MW}_1. \quad (\text{Equation S43})$$

##### (ii) Moments for intermediate products

For the intermediate products, the rate expression in Equation S38 for  $x_j$  can be rewritten as

$$dq(x_j, t)/dt = -kq(x_j, t) + 2k \int_{x_j}^\infty \frac{q(x_{j-1}, t)}{x_{j-1}} dx_{j-1}, \quad (\text{Equation S44})$$

where the subscript  $j$  explicitly denotes the degraded product with a specific chain length  $x_j$ . The formation term accounts for the generation of fragments with length  $x_j$ , which is from the fragmentation of a longer polymer chain of length  $x_{j-1}$  ( $x_j < x_{j-1} < x_0$ ). In this reaction, bond cleavage occurs randomly within the polymer chain  $x_{j-1}$ , meaning that each bond in  $x_{j-1}$  has an equal probability of  $1/x_{j-1}$  to break into  $x_j$ . When we apply the moment operation to both sides of Equation S44, yielding the equation for the intermediate products ( $1 < x_j < x_0$ )

$$\frac{d}{dt} \int_0^\infty q(x_j, t) x_j^n dx_j = -k \int_0^\infty q(x_j, t) x_j^n dx_j + 2k \int_0^\infty \left( \int_{x_j}^\infty \frac{q(x_{j-1}, t)}{x_{j-1}} dx_{j-1} \right) x_j^n dx_j, \quad (\text{Equation S45})$$

in which the second term on the right side can be rewritten by exchanging the integration order. Using Fubini's theorem (law for interchanging integration order in double integrals) of

$$\int_0^\infty \int_{x_j}^\infty f(x_{j-1}, x_j) dx_{j-1} dx_j = \int_0^\infty \int_0^{x_{j-1}} f(x_{j-1}, x_j) dx_j dx_{j-1}, \quad (\text{Equation S46})$$

we obtain

$$2k \int_0^\infty \left( \int_{x_j}^\infty \frac{q(x_{j-1}, t)}{dx_{j-1}} dx_{j-1} \right) x_j^n dx_j = 2k \int_0^\infty q(x_{j-1}, t) \left( \int_0^{x_{j-1}} \frac{x_j^n}{x_{j-1}} dx_j \right) dx_{j-1}. \quad (\text{Equation S47})$$

Using binomial expansion, the inner integral simplifies as

$$\int_0^{x_{j-1}} \frac{x_j^n}{x_{j-1}} dx_j = \frac{x_{j-1}^{n+1}}{n+1}, \quad (\text{Equation S48})$$

Thus, we obtain

$$2k \int_0^\infty \left( \int_{x_j}^\infty \frac{q(x_{j-1}, t)}{dx_{j-1}} dx_{j-1} \right) x_j^n dx_j = 2k \int_0^\infty q(x_{j-1}, t) \frac{x_{j-1}^n}{n+1} dx_{j-1}, \quad (\text{Equation S49})$$

which can be further rewritten as

$$2k \int_0^\infty \left( \int_{x_j}^\infty \frac{q(x_{j-1}, t)}{dx_{j-1}} dx_{j-1} \right) x_j^n dx_j = \frac{2k}{n+1} q_{j-1}^{(n)}(t). \quad (\text{Equation S50})$$

Inserting Equation S48 back to Equation S43, the differential equation of a specific intermediate product  $x_i$  is written as

$$dq_j^{(n)}(t)/dt = -kq_j^{(n)}(t) + \frac{2k}{n+1} q_{j-1}^{(n)}(t). \quad (\text{Equation S51})$$

With the initial conditions  $q_j^{(0)}(0) = q_j^{(1)}(0) = 0$ , we can solve the zeroth and first moments as

$$q_j^{(0)} = \frac{q^{(0)}(0)e^{-kt} (2kt)^{j-1}}{(j-1)!}, \quad (\text{Equation S52})$$

and

$$q_j^{(1)} = \frac{q^{(1)}(0)e^{-kt} (kt)^{j-1}}{(j-1)!}. \quad (\text{Equation S53})$$

### (iii) Moments for final products

For the final products, the rate expression in Equation S39 for  $x_j$  can be rewritten as

$$dr(x_j, t)/dt = 2k \int_{x_j}^\infty \frac{r(x_{j-1}, t)}{x_{j-1}} dx_{j-1}. \quad (\text{Equation S54})$$

where the subscript  $j$  ( $j = x_0 - 1$ ) denotes the degraded final product with a specific chain length  $x_j = 1$ . The formation term accounts for the generation of fragments with length  $x_j$ , which is from the fragmentation of a longer polymer chain of length  $x_{j-1}$  ( $x_j < x_{j-1} < x_0$ ). In this reaction, bond cleavage occurs randomly within the polymer chain  $x_{j-1}$ , meaning that each bond in  $x_{j-1}$  has an equal probability of  $1/x_{j-1}$  to break into  $x_j$ . When we apply the moment operation to both sides of Equation S54, yielding the equation for the final products ( $x_j = 1$ ), that is,

$$\frac{d}{dt} \int_0^\infty r(x_j, t) x_j^n dx_j = 2k \int_0^\infty \left( \int_{x_j}^\infty \frac{r(x_{j-1}, t)}{x_{j-1}} dx_{j-1} \right) x_j^n dx_j, \quad (\text{Equation S55})$$

Following the same steps as above, we obtain

$$dr_j^{(n)}(t)/dt = \frac{2k}{n+1} r_{j-1}^{(n)}(t), \quad (\text{Equation S56})$$

where the moment of intermediate product  $r_{j-1}^{(n)}(t)$  is equal to  $= q_{j-1}^{(n)}(t)$  provided above.

With the initial conditions  $r_j^{(0)}(0) = r_j^{(1)}(0) = 0$ , we can solve the zeroth and first moments as

$$r_j^{(0)} = p^{(0)}(0) \frac{(2k)^{j-1}}{(j-2)!} \left[ e^{-kt} \sum_{i=0}^{j-2} \frac{(-1)^{j-2-i} (j-2)! t^i}{i! (-k)^{j-1-i}} + \frac{1}{k^{j-1}} \right], \quad (\text{Equation S57})$$

and

$$r_j^{(1)} = p^{(1)}(0) \frac{k^{j-1}}{(j-2)!} \left[ e^{-kt} \sum_{i=0}^{j-2} \frac{(-1)^{j-2-i}(j-2)! t^i}{i! (-k)^{j-1-i}} + \frac{1}{k^{j-1}} \right]. \quad (\text{Equation S58})$$

The moments of both intermediate and final products can be calculated as

$$q^{(n)}(t) + r^{(n)}(t) = \sum_{j=1}^{x_0-2} q_j^{(n)}(t) + r_{x_0-1}^{(1)}. \quad (\text{Equation S59})$$

By taking the zeroth moment expressions in Equations S52 and S57 and the first moment expressions in Equations S53 and S59, we can derive the complete solution for all products ( $1 \leq x < x_0$ ). For long-chain polymers with high molecular weight ( $x_0 \rightarrow \infty$ ), the zeroth and first moments for all products can be simplified as

$$q^{(0)}(t) + r^{(0)}(t) = c_{\text{mole}}(0)(e^{kt} - e^{-kt}), \quad (\text{Equation S60})$$

and

$$q^{(1)}(t) + r^{(1)}(t) = c_{\text{mass}}(0)(1 - e^{-kt})\text{MW}_1 \quad (\text{Equation S61})$$

### 3. Number-average molecular weight

Therefore, the total molar concentration as a summation of  $p^{(0)}(t)$ ,  $q^{(0)}(t)$ ,  $r^{(0)}(t)$  is equal to

$$c_{\text{mole}}(t) = c_{\text{mole}}(0)e^{kt}. \quad (\text{Equation S62})$$

Therefore, the total mass concentration as a summation of  $p^{(1)}(t)\text{MW}_1$ ,  $q^{(1)}(t)\text{MW}_1$ ,  $r^{(1)}(t)\text{MW}_1$  is equal to

$$c_{\text{mass}}(t) = c_{\text{mass}}(0). \quad (\text{Equation S63})$$

The number-average MW is defined as the ratio of total mass concentration to total molar concentration, that is

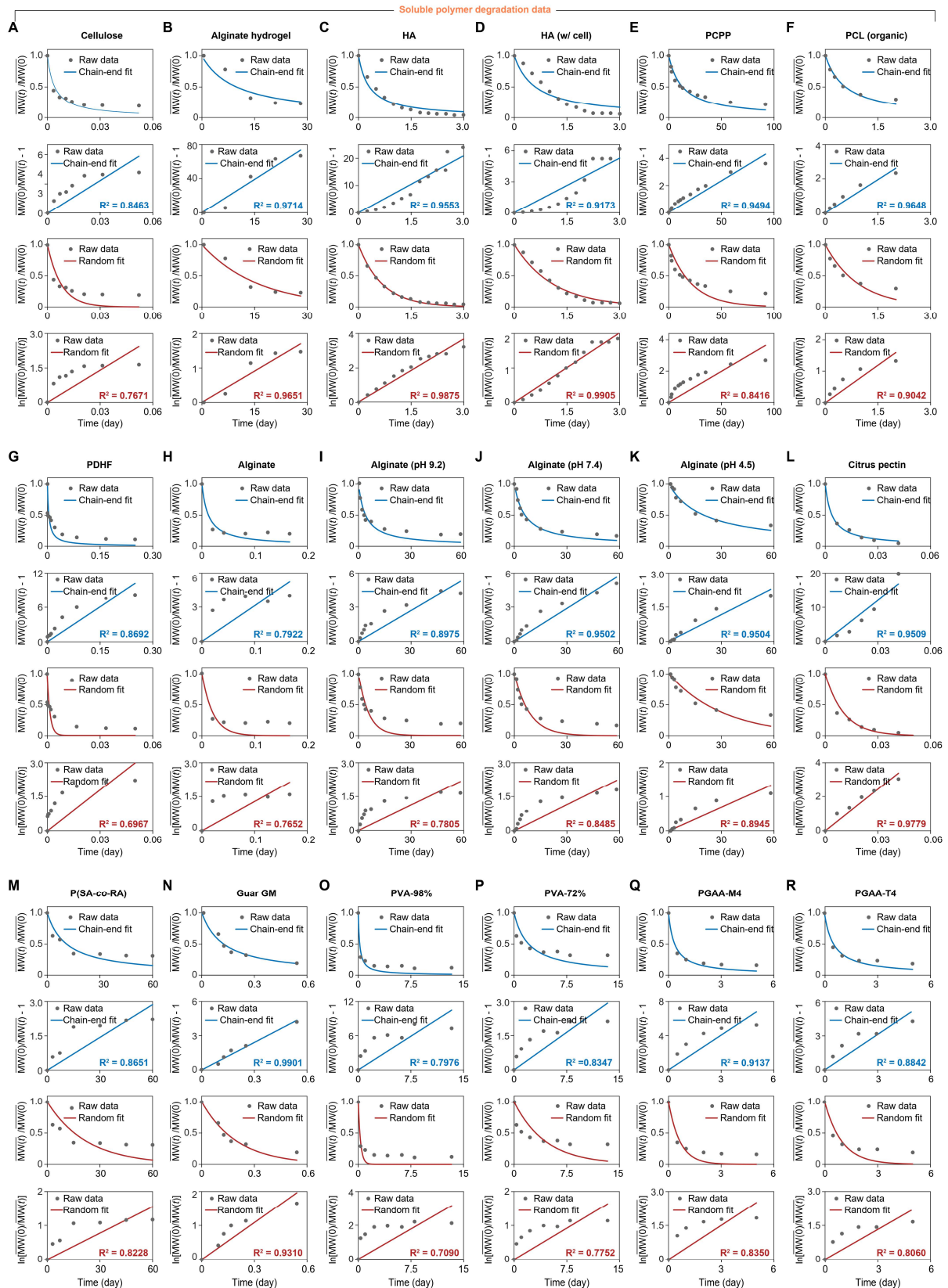
$$\overline{\text{MW}(t)} = \overline{\text{MW}(0)}e^{-kt}. \quad (\text{Equation S64})$$

This expression provides a mathematical description of MW decay kinetics under random scission. Additionally, we plot the normalized molar concentrations and normalized mass concentrations over time in **Figure S3A, B**, based on the above expressions for both undegraded reactants and degraded products. For the graphs in **Figure 2F-H** and **Figure S3A,B**, we assume the following values for a polydisperse polymer sample:  $c_{\text{mole}}(0) = 1 \text{ mmol L}^{-1}$ ,  $c_{\text{mass}}(0) = 5 \text{ g L}^{-1}$ ,  $\text{MW}_1 = 100 \text{ g mol}^{-1}$ .

**Note S4. Calculation of the degradable bond fraction.**

The fraction of degradable bonds per repeat unit is defined as the ratio of the number of degradable bonds (e.g., ester, ether, glycosidic bonds) to the total number of covalent bonds along the polymer backbone within a single repeat unit. The total bond number includes both degradable and non-degradable bonds (e.g., C–C, C–O, C–N). For PLA, the main backbone consists of three covalent bonds (i.e., two shared and two owned, calculated as  $2 \times 0.5 + 2 = 3$ , marked in blue and red). Among these, one ester bond is hydrolytically degradable (marked in red). Therefore, the fraction of degradable bonds per repeat unit in PLA is  $1/3 \approx 0.3$  (**Figure S5A**). For polymers with ring-containing repeat units (e.g., pyranose ring in alginate or aromatic ring in PET), the number of backbone bonds is determined using the shortest path principle, ensuring that only covalent bonds contributing to the continuous chain structure are counted. As illustrated in **Figure S5B**, a ring-containing repeat unit with a citrus pectin backbone is composed of ten covalent bonds (marked in blue and red), including two ether bonds (marked in red). This gives a degradable bond fraction of  $2/10 = 0.2$ . This degradable bond fraction serves as a simplified quantitative parameter to describe the intrinsic degradability of a polymer backbone, providing a consistent way to compare different polymers based on their chemical structure.

## Supplemental Figures



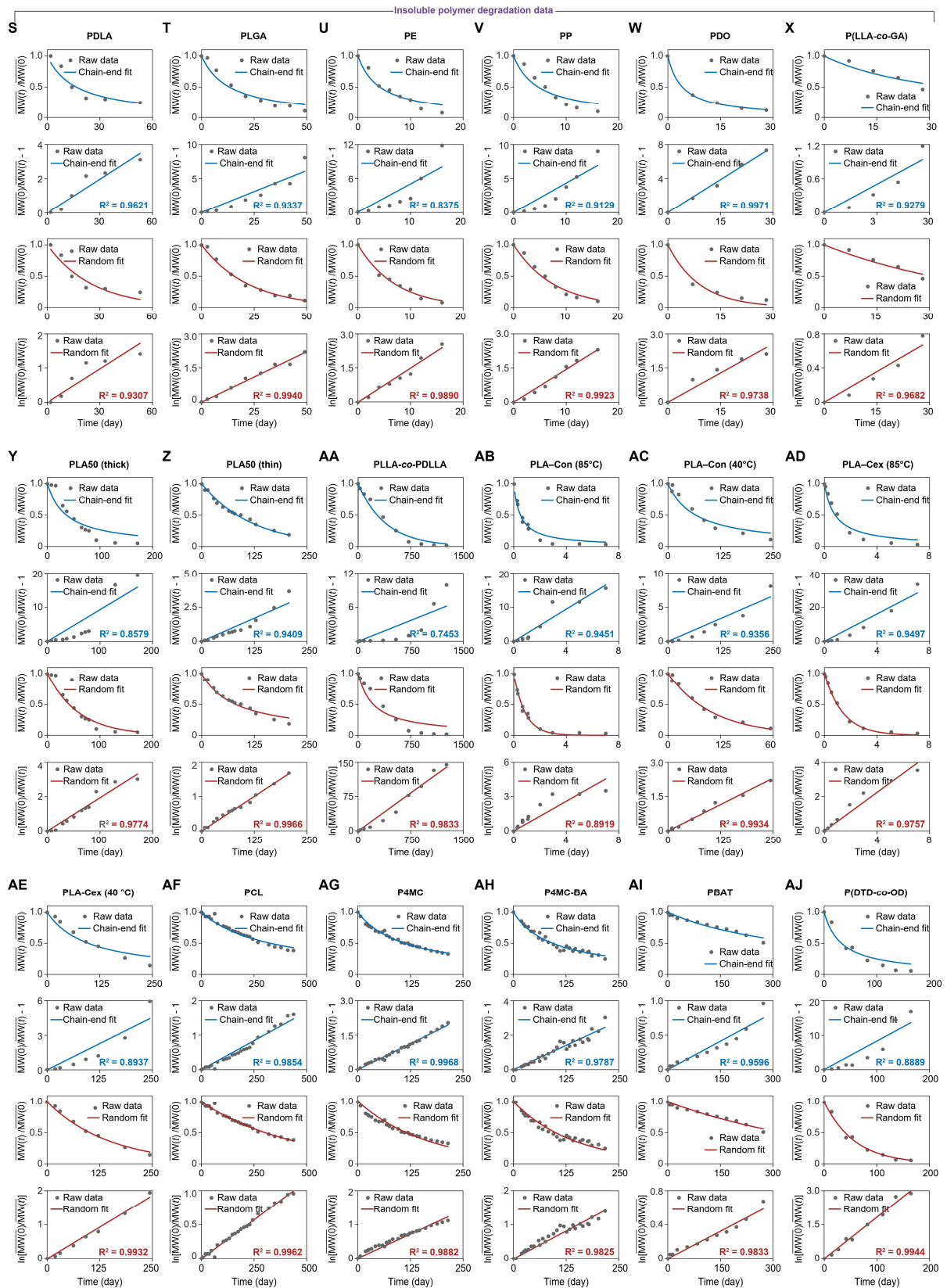


**Figure S1. Fitting polymer degradation data to chain scission modes.** The compiled data for all 41 polymers with different polymer types and degradation conditions were plotted using normalized MW decay over time. For the three selected soluble polymers (e.g., chitosan[S3], dextran[S4], PLA-co-PEG[S5]) and three insoluble polymers (e.g., PLA[S6], PLGA[S7], PET[S8]), normalized MW decay over time was plotted in **Figure 3** of the main text. The experimental data of MW decay over time for **(A)** cellulose[S9], **(B)** alginate hydrogel[S10], **(C)** hyaluronic acid (HA)[S11], **(D)** hyaluronic acid in cell culture (HA (w/cell)) [S11], **(E)** poly[di(carboxylatophenoxy)phosphazene] (PCPP)[S12], **(F)** polycaprolactone dissolved in organic solvent (PCL (organic))[S13], **(G)** poly(2,5-dihydrofuran) (PDHF)[S14], **(H)** alginate[S15], **(I)** alginate (pH 9.2)[S16], **(J)** alginate (pH 7.4)[S16], **(K)** alginate (pH 4.5)[S16], **(L)** citrus pectin[S17], **(M)** poly (sebacic acid-co-ricinoleic acid) (P(SA-co-RA))[S18], **(N)** guar galactomannan (Guar GM)[S19], **(O)** 98% hydrolyzed polyvinyl alcohol (PVA-98%)[S20], **(P)** 72% hydrolyzed polyvinyl alcohol (PVA-72%)[S20], **(Q)** poly(glycoamidoamine) with D-mannaramide (PGAA M4)[S21], **(R)** poly(glycoamidoamine) with L-tartaramide (PGAA T4)[S21], **(S)** poly(D,L-lactide) (PDLA)[S22], **(T)** poly (lactic-co-glycolic acid) (PLGA)[S7], **(U)** polyethylene (PE)[S23], **(V)** polypropylene (PP)[S23], **(W)** polydioxanone (PDO)[S24], **(X)** poly(L-lactide-co-glycolide) (P(LLA-co-GA))[S24], **(Y)** polylactic acid thick sample (PCL(thick))[S25], **(Z)** polylactic acid thin sample (PCL(thin))[S25], **(AA)** poly(L-lactide)-co-poly(D,L-lactide) (PLLA-co-PDLLA)[S26], **(AB)** neat polylactic acid at 85°C (PLA-Con (85°C))[S27], **(AC)** neat polylactic acid at 40°C (PLA-Con (40°C))[S27], **(AD)** polylactic acid with chain extender (PLA-Cex (85°C))[S27], **(AE)** polylactic acid with chain extender (PLA-Cex (85°C))[S27], **(AF)** polycaprolactone (PCL)[S28], **(AG)** poly(4-methylcaprolactone) (P4MC)[S28], **(AH)** poly(4-methylcaprolactone) with benzyl alcohol (P4MC-BA)[S28], **(AI)** polybutylene adipate-co-terephthalate (PBAT)[S29], and **(AJ)** poly(desaminotyrosyl-tyrosine dodecyl dodecanedioate) (P(DTD-co-OD))[S30] are fitted to chain-end scission (blue line) and random scission (red line) models.

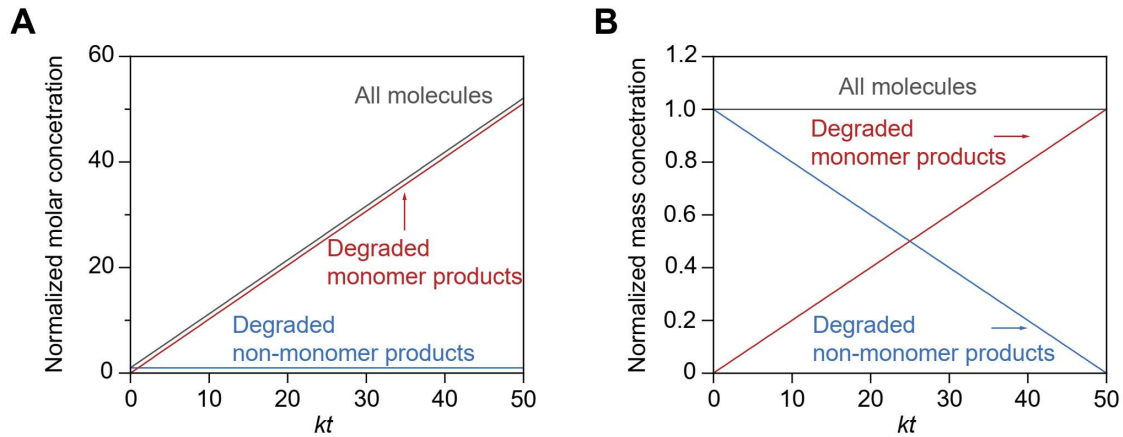


**Figure S2. Time evolution of normalized molar and mass concentrations under chain-end scission.** **(A)** Normalized molar concentrations (zeroth moments) for all molecules, degraded non-monomer products (chain length of  $x_0 - 1$ ), and degraded monomer products (chain length of 1). **(B)** Normalized mass concentrations (first moments) for all molecules, degraded non-monomer products (chain length of  $x_0 - 1$ ), and degraded monomer products (chain length of 1).

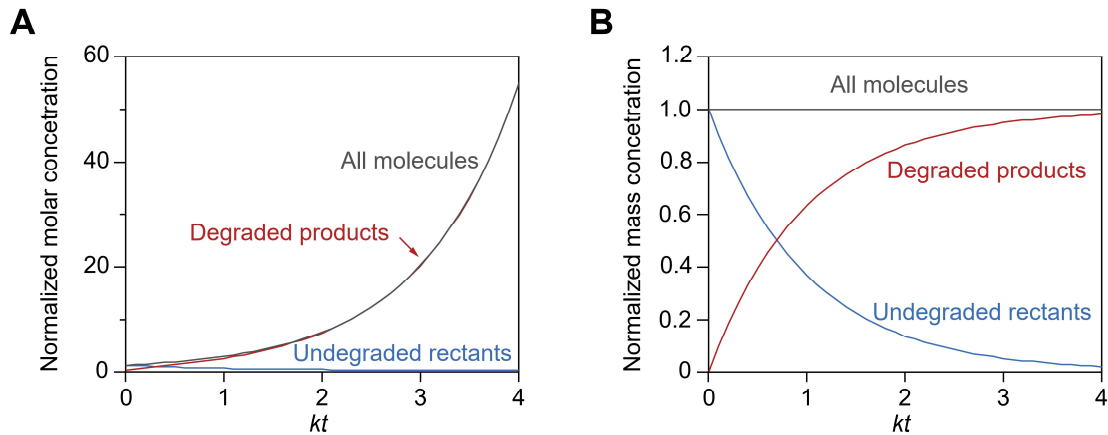


**Figure S3. Time evolution of normalized molar and mass concentrations under random scission.** **(A)** Normalized molar concentrations (zeroth moments) for all molecules, undegraded reactants (chain length =  $x_0$ ), and degraded products (chain length  $< x_0$ ). **(B)** Normalized mass concentrations (first moments) for all molecules, undegraded reactants (chain length =  $x_0$ ), and degraded products (chain length  $< x_0$ ).

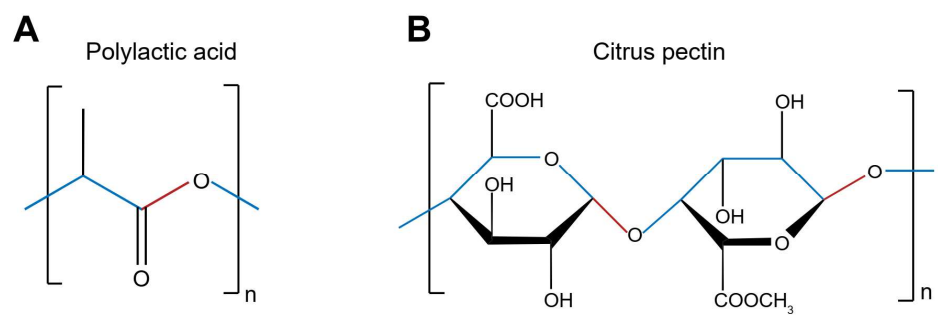


**Figure S4. Chemical structures of representative degradable polymers.** Examples: (a) polylactic acid (PLA) and (b) citrus pectin.

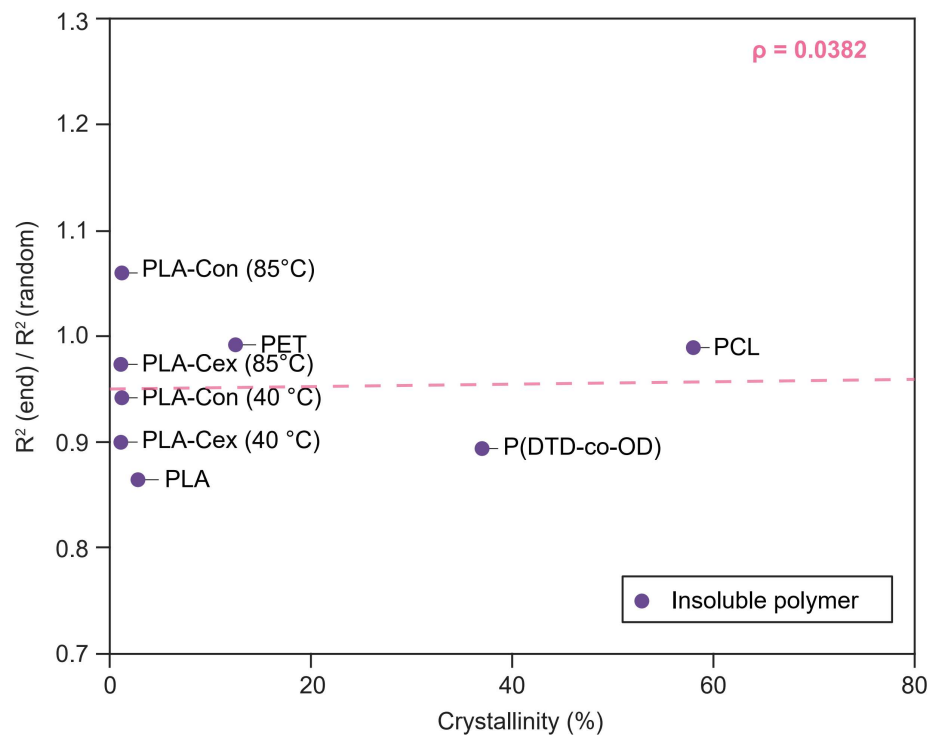


**Figure S5. Pearson correlation analysis of polymer crystallinity with chain scission preference.** The ratio of  $R^2(\text{end})$  to  $R^2(\text{random})$  is plotted against polymer crystallinity. Pearson correlation coefficient ( $\rho$ ) is indicated.

**Supplemental Tables**

**Table S1. Summary of different polymer degradation with chain scission fitting and polymer characteristics.**

No.	Polymer	Full chemical name	R <sup>2</sup> (random)	R <sup>2</sup> (end)	R <sup>2</sup> (end)/R <sup>2</sup> (chain)	Initial MW (kDa)	Deg. bond fraction	Catalyst	Catalyst size (nm)	Solubility (g per g solvent)	Deg. timescale 1/k (day)	Ref.
1	Chitosan	Chitosan	0.8818	0.9974	1.1311	213.00	0.200	Hydrogen peroxide	0.36	0.0050	0.006	S3
2	Dextran	Dextran	0.9040	0.9863	1.0910	875.30	0.200	Dextranase	6	0.0100	0.00	S4
3	PLA-co-PEG	Poly(ethylene glycol)-co-polylactide methyl ether	0.8257	0.9546	1.1561	32.64	0.333	H <sub>2</sub> O	0.28	0.0020	2.75	S5
4	Cellulose	Cellulose	0.7671	0.8463	1.1032	386.62	0.200	H <sup>+</sup> /H <sub>2</sub> O	0.28	0.0010	0.01	S9
5	Alginate hydrogel	Alginate	0.9651	0.9714	1.0065	115.66	0.200	H <sub>2</sub> O	0.28	0.0300	16.16	S10
6	HA	Hyaluronic acid	0.9875	0.9553	0.9674	1876.40	0.222	Hyaluronidase	7	0.0050	0.68	S11
7	HA (w/cell)	Hyaluronic acid	0.9905	0.9173	0.9261	1882.02	0.222	Hyaluronidase	7	0.0050	1.10	
8	PCPP	Poly[di(carboxylatophenoxy)phosphazene]	0.8416	0.9494	1.1281	820.00	1.000	H <sub>2</sub> O	0.28	0.0040	21.93	S12
9	PCL (organic)	Polycaprolactone	0.9042	0.9648	1.0670	11.67	0.143	H <sub>2</sub> O	0.28	0.0020	0.95	S13
10	PDHF	Poly(2,5-dihydrofuran)	0.6967	0.8692	1.2476	44.52	0.200	Grubbs catalysts	2	0.0052	0.01	S14
11	Alginate	Alginate	0.7652	0.7922	1.0353	345.78	0.200	Hydrogen peroxide	0.36	0.0100	0.02	S15
12	Alginate (pH 9.2)	Alginate	0.7805	0.8975	1.1499	114.35	0.200	H <sub>2</sub> O	0.28	0.0200	5.69	S16
13	Alginate (pH 7.4)	Alginate	0.8485	0.9502	1.1199	149.58	0.200	H <sub>2</sub> O	0.28	0.0200	8.61	
14	Alginate (pH 4.5)	Alginate	0.8945	0.9504	1.0625	220.71	0.200	H <sub>2</sub> O	0.28	0.0200	31.06	

No.	Polymer	Full chemical name	R <sup>2</sup> (random)	R <sup>2</sup> (end)	R <sup>2</sup> (end)/R <sup>2</sup> (chain )	Initial MW (kDa)	Deg. bond fraction	Catalyst	Catalyst size (nm)	Solubility (g per g solvent)	Deg. timescale 1/k (day)	Ref.
15	Citrus pectin	Citrus pectin	0.9779	0.9509	0.9724	451.48	0.200	Hydrogen peroxide, Fe <sup>3+</sup>	0.36	0.0050	0.01	S17
16	P(SA-co-RA)	Poly(sebacic acid-co-ricinoleic acid)	0.8228	0.8651	1.0514	3.49	0.083	H <sub>2</sub> O	0.28	0.0040	22.32	S18
17	Guar GM	Guar galactomannan	0.9310	0.9911	1.0646	1790.00	0.200	Endo-β-mannanase	3.8	0.0100	0.20	S19
18	PVA-98%	Polyvinyl alcohol, 98% hydrolyzed	0.7090	0.7976	1.1249	36.17	0.500	Microbe	6	0.0042	0.33	S20
19	PVA-72%	Polyvinyl alcohol, 72% hydrolyzed	0.7752	0.8347	1.0767	13.52	0.500	Microbe	6	0.0042	4.46	
20	PGAA-M4	Poly(glycoamidoamine) with D-mannaramide	0.8350	0.9137	1.0942	4.90	0.095	H <sub>2</sub> O	0.28	0.0245	0.97	S21
21	PGAA-T4	Poly(glycoamidoamine) with L-tartaramide	0.8060	0.8842	1.0970	5.60	0.105	H <sub>2</sub> O	0.28	0.0280	0.65	
22	PLA	Polylactic acid	0.9983	0.8630	0.8645	11.67	0.333	H <sub>2</sub> O	0.28	1E-06	7.87	S6
23	PLGA	Poly(lactic-co-glycolic acid)	0.9940	0.9337	0.9393	4.39	0.333	H <sub>2</sub> O	0.28	1E-06	22.47	S7
24	PET	Polyethylene terephthalate	0.9915	0.9834	0.9918	26.74	0.200	H <sub>2</sub> O	0.28	1E-06	13.76	S8
25	PDLA	Poly(D,L-lactide)	0.9307	0.9621	1.0337	1156.54	0.333	H <sub>2</sub> O	0.28	1E-06	25.77	S22
26	PE	Polyethylene	0.9890	0.8375	0.8468	Unknown	0.500	Microbe	10	1E-06	7.17	S23
27	PP	Polypropylene	0.9923	0.9129	0.9200	Unknown	0.500	Microbe	10	1E-06	7.67	
28	PDO	Polydioxanone	0.9738	0.9971	1.0239	Unknown	0.167	OH <sup>-</sup> /H <sub>2</sub> O	0.28	1E-06	9.06	S24
29	P(LLA-co-GA)	Poly(L-lactide-co-glycolide)	0.9687	0.9279	0.9579	Unknown	0.333	OH <sup>-</sup> /H <sub>2</sub> O	0.28	1E-06	44.44	

No.	Polymer	Full chemical name	R <sup>2</sup> (random)	R <sup>2</sup> (end)	R <sup>2</sup> (end)/R <sup>2</sup> (chain )	Initial MW (kDa)	Deg. bond fraction	Catalyst	Catalyst size (nm)	Solubility (g per g solvent)	Deg. timescale 1/k (day)	Ref.
30	PLA50 (thick)	Polylactic acid	0.9774	0.8579	0.8777	43.00	0.333	H <sub>2</sub> O	0.28	1E-06	58.02	S25
31	PLA50 (thin)	Polylactic acid	0.9966	0.9409	0.9441	67.00	0.333	H <sub>2</sub> O	0.28	1E-06	119.25	
32	PLLA-co-PDLLA	Poly(L-lactide)-co-poly(D, L-lactide)	0.9833	0.7453	0.7580	95.12	0.167	H <sub>2</sub> O	0.28	1E-06	400.00	S26
33	PLA-Con (85°C)	Polylactic acid	0.8919	0.9451	1.0596	106.10	0.333	H <sub>2</sub> O	0.28	1E-06	0.87	S27
34	PLA-Con (40°C)	Polylactic acid	0.9934	0.9356	0.9418	106.30	0.333	H <sub>2</sub> O	0.28	1E-06	105.26	
35	PLA-Cex (85°C)	Polylactic acid	0.9757	0.9497	0.9734	191.60	0.333	H <sub>2</sub> O	0.28	1E-06	1.40	
36	PLA-Cex (40°C)	Polylactic acid	0.9932	0.8937	0.8998	191.60	0.333	H <sub>2</sub> O	0.28	1E-06	147.06	
37	PCL	Polycaprolactone	0.9962	0.9854	0.9892	31.47	0.333	H <sub>2</sub> O	0.28	1E-06	434.78	S28
38	P4MC	Poly(4-methylcaprolactone)	0.9882	0.9968	1.0087	21.84	0.143	H <sub>2</sub> O	0.28	1E-06	163.93	
39	P4MC-BA	Poly(4-methylcaprolactone) with benzyl alcohol	0.9825	0.9787	0.9961	14.61	0.143	H <sub>2</sub> O	0.28	1E-06	144.93	
40	PBAT	Polybutylene adipate-co-terephthalate	0.9833	0.9596	0.9758	88.39	0.167	Microbe	20	1E-06	473.83	S29
41	P(DTD-co-OD)	Poly(desaminotyrosyl-tyrosine dodecyl dodecanedioate)	0.9944	0.8889	0.8939	59.00	0.107	H <sub>2</sub> O	0.28	1E-06	57.66	S30

**Table S2. Summary of different polymer degradation with chain scission fitting and polymer crystallinity.**

No.	Polymer	R <sup>2</sup> (end)/R <sup>2</sup> (chain)	Crystallinity (%)	Ref.
1	PLA	0.8645	59.50	S6
2	PET	0.9918	12.50	S8
3	PLA-Con (85°C)	1.0596	37.25	S27
4	PLA-Con (40°C)	0.9418	7.85	
5	PLA-Cex (85°C)	0.9734	77.70	
6	PLA-Cex (40°C)	0.8998	6.90	
7	PCL	0.9892	66.00	S28
8	P(DTD-co-OD)	0.8939	54.50	S30

### **Supplemental References**

- [S1] McCoy, B.J., and Madras, G. (2004). Degradation kinetics of polymers in solution: Dynamics of molecular weight distributions. *AIChE J.* **43**, 802-810.
- [S2] Wang, M., Smith, J., and McCoy, B.J. (1995). Continuous kinetics for thermal degradation of polymer in solution. *AIChE Journal* **41**, 1521-1533.
- [S3] Chang, K.L.B., Tai, M.-C., and Cheng, F.-H. (2001). Kinetics and products of the degradation of chitosan by hydrogen peroxide. *Journal of Agricultural and Food Chemistry* **49**, 4845-4851.
- [S4] Wang, Q., Liu, T., Xu, X., Chen, H., and Chen, S. (2021). Dextran degradation by sonoenzymolysis: Degradation rate, molecular weight, mass fraction, and degradation kinetics. *International Journal of Biological Macromolecules* **169**, 60-66.
- [S5] Kucharczyk, P., Pavelková, A., Stloukal, P., and Sedlářík, V. (2016). Degradation behaviour of PLA-based polyesterurethanes under abiotic and biotic environments. *Polymer Degradation and Stability* **129**, 222-230.
- [S6] Stloukal, P., Jandikova, G., Koutny, M., and Sedlářík, V. (2016). Carbodiimide additive to control hydrolytic stability and biodegradability of PLA. *Polymer Testing* **54**, 19-28.
- [S7] Li, J., Nemes, P., and Guo, J. (2018). Mapping intermediate degradation products of poly (lactic-co-glycolic acid) in vitro. *Journal of Biomedical Materials Research Part B: Applied Biomaterials* **106**, 1129-1137.
- [S8] Launay, A., Thominette, F., and Verdu, J. (1999). Hydrolysis of poly (ethylene terephthalate). A steric exclusion chromatography study. *Polymer degradation and stability* **63**, 385-389.
- [S9] Härdelin, L., Perzon, E., Hagström, B., Walkenström, P., and Gatenholm, P. (2013). Influence of molecular weight and rheological behavior on electrospinning cellulose nanofibers from ionic liquids. *Journal of Applied Polymer Science* **130**, 2303-2310.
- [S10] Kong, H.J., Kaigler, D., Kim, K., and Mooney, D.J. (2004). Controlling rigidity and degradation of alginate hydrogels via molecular weight distribution. *Biomacromolecules* **5**, 1720-1727.
- [S11] Mei, J., Dong, Z., Yi, Y., Zhang, Y., and Ying, G. (2019). A simple method for the production of low molecular weight hyaluronan by in situ degradation in fermentation broth. *e-Polymers* **19**, 477-481.
- [S12] Andrianov, A.K., Svirkin, Y.Y., and LeGolvan, M.P. (2004). Synthesis and biologically relevant properties of polyphosphazene polyacids. *Biomacromolecules* **5**, 1999-2006.
- [S13] Hoskins, J.N., and Grayson, S.M. (2009). Synthesis and degradation behavior of cyclic poly ( $\epsilon$ -caprolactone). *Macromolecules* **42**, 6406-6413.
- [S14] Hsu, T.-G., Liu, S., Guan, X., Yoon, S., Zhou, J., Chen, W.-Y., Gaire, S., Seylar, J., Chen, H., and Wang, Z. (2023). Mechanochemically accessing a challenging-to-synthesize depolymerizable polymer. *Nature Communications* **14**, 225.
- [S15] Mao, S., Zhang, T., Sun, W., and Ren, X. (2012). The depolymerization of sodium alginate by oxidative degradation. *Pharmaceutical development and technology* **17**, 763-769.
- [S16] Bouhadir, K.H., Lee, K.Y., Alsberg, E., Damm, K.L., Anderson, K.W., and Mooney, D.J. (2001). Degradation of partially oxidized alginate and its potential application for tissue engineering. *Biotechnology progress* **17**, 945-950.
- [S17] Zhi, Z., Chen, J., Li, S., Wang, W., Huang, R., Liu, D., Ding, T., Linhardt, R.J., Chen, S., and Ye, X. (2017). Fast preparation of RG-I enriched ultra-low molecular weight pectin by an ultrasound accelerated Fenton process. *Scientific Reports* **7**, 541.
- [S18] Ickowicz, D.E., Abtew, E., Khan, W., Golovanevski, L., Steinman, N., Weiniger, C.F., and Domb, A.J. (2016). Poly (ester-anhydride) for controlled delivery of hydrophilic drugs. *Journal of Bioactive and Compatible Polymers* **31**, 127-139.

- [S19] Tayal, A., and Khan, S.A. (2000). Degradation of a water-soluble polymer: molecular weight changes and chain scission characteristics. *Macromolecules* 33, 9488-9493.
- [S20] Solaro, R., Corti, A., and Chiellini, E. (2000). Biodegradation of poly (vinyl alcohol) with different molecular weights and degree of hydrolysis. *Polymers for Advanced Technologies* 11, 873-878.
- [S21] Liu, Y., and Reineke, T.M. (2010). Degradation of poly (glycoamidoamine) DNA delivery vehicles: polyamide hydrolysis at physiological conditions promotes DNA release. *Biomacromolecules* 11, 316-325.
- [S22] Park, T.G. (1994). Degradation of poly (D, L-lactic acid) microspheres: effect of molecular weight. *Journal of Controlled Release* 30, 161-173.
- [S23] Zhou, J., Li, L., Wang, D., Wang, L., Zhang, Y., and Feng, S. (2022). Study on Rapid Detection Method for Degradation Performance of Polyolefin-Based Degradable Plastics. *Polymers* 15, 183.
- [S24] Reske, T., Eickner, T., Grabow, N., Schmitz, K.-P., and Siewert, S. (2020). Accelerated Degradation of polymeric surgical suture materials. *Current Directions in Biomedical Engineering* 6, 458-460.
- [S25] Grizzi, I., Garreau, H., Li, S., and Vert, M. (1995). Hydrolytic degradation of devices based on poly (DL-lactic acid) size-dependence. *Biomaterials* 16, 305-311.
- [S26] Otsuka, F., Pacheco, E., Perkins, L.E., Lane, J.P., Wang, Q., Kamberi, M., Frie, M., Wang, J., Sakakura, K., and Yahagi, K. (2014). Long-term safety of an everolimus-eluting bioresorbable vascular scaffold and the cobalt-chromium XIENCE V stent in a porcine coronary artery model. *Circulation: Cardiovascular Interventions* 7, 330-342.
- [S27] Limsukon, W., Auras, R., and Selke, S. (2019). Hydrolytic degradation and lifetime prediction of poly (lactic acid) modified with a multifunctional epoxy-based chain extender. *Polymer Testing* 80, 106108.
- [S28] Antheunis, H., van der Meer, J.-C., de Geus, M., Kingma, W., and Koning, C.E. (2009). Improved mathematical model for the hydrolytic degradation of aliphatic polyesters. *Macromolecules* 42, 2462-2471.
- [S29] Kijchavengkul, T., Auras, R., Rubino, M., Alvarado, E., Montero, J.R.C., and Rosales, J.M. (2010). Atmospheric and soil degradation of aliphatic–aromatic polyester films. *Polymer Degradation and Stability* 95, 99-107.
- [S30] Miles, C.E., Lima, M.R.N., Buevich, F., Gwin, C., Sanjeeva Murthy, N., and Kohn, J. (2021). Comprehensive hydrolytic degradation study of a new poly(ester-amide) used for total meniscus replacement. *Polymer Degradation and Stability* 190, 109617.